

A mass estimate of an intermediate-mass black hole in ω Centauri

P. Miocchi

INAF, Osservatorio Astronomico di Bologna, and Dipartimento di Astronomia, Università di Bologna,
via Ranzani 1, Bologna 40127, Italy
e-mail: paolo.miocchi@unibo.it

Received 4 July 2009 / Accepted 8 February 2010

ABSTRACT

Context. The problem of the existence of intermediate-mass black holes (IMBHs) at the centre of globular clusters is a hot and controversial topic in current astrophysical research with important implications in stellar and galaxy formation.

Aims. The purpose of this paper is to provide further evidence on the presence of an IMBH in ω Centauri and to give an independent estimate of its mass.

Methods. We employed a self-consistent spherical model with anisotropic velocity distribution. It consists in a generalisation of the King model by including the Bahcall-Wolf distribution function in the IMBH vicinity.

Results. By the parametric fitting of the model to recent HST/ACS data for the surface brightness profile, we found an IMBH to cluster total mass ratio of $M_{\bullet}/M = 5.8_{-1.2}^{+0.9} \times 10^{-3}$. It is also found that the model yields a fit of the line-of-sight velocity dispersion profile that is better without mass segregation than in the segregated case. This confirms the current thought of a non-relaxed status for this peculiar cluster. The best fit model to the kinematic data leads, moreover, to a cluster total mass estimate of $M = (3.1 \pm 0.3) \times 10^6 M_{\odot}$, thus giving an IMBH mass in the range $1.3 \times 10^4 < M_{\bullet} < 2.3 \times 10^4 M_{\odot}$ (at 1σ confidence level). A slight degree of radial velocity anisotropy in the outer region ($r \gtrsim 12'$) is required to match the outer surface brightness profile.

Key words. black hole physics – methods: analytical – methods: numerical – Galaxy: kinematics and dynamics – globular clusters: individual: ω Centauri (NGC 5139) – stars: kinematics and dynamics

1. Introduction

Intermediate-mass black holes (IMBH) still belong to the class of “exotic” objects in the current astrophysical belief. With a mass $M_{\bullet} \sim 100\text{--}10^4 M_{\odot}$, they would represent the minor mass counterpart of super-massive black holes – whose existence is established with much more robustness – but still more massive than stellar black holes. One of the places where they should more likely be located is among the densest stellar environments in the Universe, i.e. at the globular clusters (GCs) centre. However, so far, the most direct observable signature of their existence, namely the emission in the radio and X-ray bands (mainly from Bondi-Hoyle accretion of intracluster gas), is not yet really clear and conclusive (see, e.g., Liu & Di Stefano 2008; Zepf et al. 2008; Irwin et al. 2010; Strohmayr & Mushotzky 2009; and Miller & Colbert 2004, for a general review).

To date, only the GC G1 (in M 31) exhibits a detected source, seen in both radio (with an 8.4 GHz power of $2 \times 10^{15} \text{ W Hz}^{-1}$, see Ulvestad et al. 2007) and X-ray (with a $2 \times 10^{36} \text{ erg s}^{-1}$ luminosity at 0.2–10 keV, see Pooley & Rappaport 2006) bands. The observed fluxes, as well as their ratio, are compatible with the claimed presence of a $\sim 2 \times 10^4 M_{\odot}$ IMBH (Gebhardt et al. 2005) – although other kinds of sources cannot be completely ruled out (e.g. Kong et al. 2009). Another extra-galactic hyper-luminous X-ray source ($5\text{--}100 \times 10^{40} \text{ erg s}^{-1}$ at 0.3–10 keV) is located in the S0-a galaxy ESO243-49 and its features suggest an IMBH emission. Recently, an unresolved optical counterpart with brightness comparable to that of a massive GC has been identified around this source (Soria et al. 2010), though higher resolution observations are needed.

In our Galaxy, the central region of NGC 6388 hosts an unresolved set of X-ray sources, with a total luminosity of $2.7 \times 10^{33} \text{ erg s}^{-1}$ (Nucita et al. 2008), implying an accretion efficiency compatible with the inferred presence of a $\sim 6 \times 10^3 M_{\odot}$ IMBH (Lanzoni et al. 2007). On the other hand, no detectable X-ray sources have been found at the centre of mass of NGC 2808, leading Servillat et al. (2008) to state that $M_{\bullet} \lesssim 290 M_{\odot}$ in this cluster.

In fact, in most cases only upper limits for IMBHs masses can be deduced from radio observations (see, e.g. Maccarone & Servillat 2008, for NGC 2808 and for a general discussion). These surprisingly low upper limits lead Maccarone & Servillat (2008) to cast doubts on the fact that the scaling relation $M_{\bullet} - \sigma$, where σ is the central velocity dispersion of the host stellar system (with mass M and luminosity L), is the same $M_{\bullet} \sim \sigma^{4.8}$ law that has been clearly noted for super-massive black holes in galaxies (Ferrarese & Merritt 2000; Gebhardt et al. 2000). It should be emphasised, however, that the upper limits on IMBH masses drawn from X-ray or radio observations strongly depend on the assumption that the gas distribution around the compact object is uniform (isotropic accretion). It is clear that, if this distribution had any amount of clumpiness, those limits could be largely underestimated.

Nevertheless, the question of the validity of the extrapolation of the $M_{\bullet} - \sigma$ scaling relation to IMBHs is still open and deserves to be discussed briefly here. In general, this relation can be understood as a consequence of the fundamental scaling law $M_{\bullet} \propto M$ (Magorrian et al. 1998). In galaxies, this scaling law and the two relations $M \sim L^{5/4}$ (Faber et al. 1987) and $L \sim \sigma^4$ (Faber & Jackson 1976), lead just to $M_{\bullet} \sim \sigma^5$. In

globular clusters, on the other hand, the observed trends are $M \sim L$ and $L \sim \sigma^{5/3}$ (Meylan & Heggie 1997), which in fact yield $M_{\bullet} \sim \sigma^{1.7}$. This implies a generally lower mass ratio between the IMBH and the host cluster, as noted by Maccarone & Servillat (2008). A shallow $M_{\bullet} - \sigma$ relation, namely $M_{\bullet} \sim \sigma^{1.2}$, was already reported in Mocchi (2007, hereafter M07) based on parametric IMBH mass estimates (see below). On the other hand, we must mention a recent study of this specific topic, in which the low-mass extrapolation of the galactic $M_{\bullet} \sim \sigma^{4.8}$ relation seems to fit a sample of 5 reported IMBHs in GCs (Safonova & Shastri 2010).

In view of all this, the study of possible IMBH fingerprints on either star-count or surface brightness (SB) profiles is a detection route that still deserves to be pursued, especially when kinematic observations close to the IMBH gravitational influence region are available. In this respect, a spherical and self-consistent model of GCs with a central IMBH at rest was presented in M07, both with equal mass stars, i.e. the single-mass (SM) case, and with a multimass (MM) stellar spectrum including mass segregation. This model is an extension of King-Michie models (Michie 1963; Michie & Bodenheimer 1963; King 1966) that is obtained by including the Bahcall-Wolf stellar distribution function within the IMBH gravitational influence region. The latter was shown to solve the Fokker-Planck equation in the vicinity of a central IMBH that formed long before a cluster relaxation time (Bahcall & Wolf 1976; Binney & Tremaine 1987), and its validity was subsequently confirmed by accurate numerical simulations (Freitag & Benz 2002; Baumgardt et al. 2004; Preto et al. 2004).

The typical SB profile that comes out of the model has, for any reasonable IMBH mass, the appearance of a normal low- or medium-concentration cluster ($c \lesssim 2$) and shows a steep cusp only in the very inner region (typically within a tenth of the core radius) delimited by the “cusp radius”, r_{cu} . In fact, outside r_{cu} , a shallow power-law behaviour – with a logarithmic slope $s \lesssim 0.25$ – is the most easily observable fingerprint in the otherwise flat core profile. Interestingly, this confirmed the finding of other authors who – using a completely different approach (accurate N -body simulations) – also claim that IMBHs most likely reside in non-core-collapsed clusters showing just a weak rise of the SB in the core region (Baumgardt et al. 2005; Trenti et al. 2007). Recently, high-resolution Montecarlo simulations have provided another independent confirmation of these structural features (Umbreit et al. 2009). On the other hand, according to other N -body experiments, it is claimed that post-core-collapsed GCs also exhibit a King-like profile, but with a $s \sim 0.4$ – 0.7 steep core behaviour (Trenti et al. 2010); it must be emphasised, however, that M07 models yield core profiles that are always significantly flatter and unable to fit behaviours with such a high s .

The shape of the SB profile given by the M07 model depends on 2 dimensionless parameters¹. For the purposes of this study, we use the IMBH to cluster mass ratio, M_{\bullet}/M , and the dimensionless gravitational potential at the edge of the IMBH dynamical influence region, W_{BH} . The latter replaces the usual King model’s central dimensionless potential W_0 , with the aim of avoiding the singularity at the cluster centre in the presence of the IMBH (see M07, for further details).

In M07 it was shown that lower and upper limits of M_{\bullet} exist as a function of c and s . This relationship was then applied to investigate the presence of IMBHs in the set of GCs, whose

SB was accurately measured in Noyola & Gebhardt (2006) using HST/WFPC2 archive images. Among the six candidate clusters found, NGC 6388 and M54 have subsequently been the objects of further and more detailed studies (through parametric fitting of star-count profiles) that suggest the presence of an IMBH with mass $\sim 6 \times 10^3 M_{\odot}$ in the former (Lanzoni et al. 2007) and $\sim 10^4 M_{\odot}$ in the latter (Ibata et al. 2009, in this case kinematic data were also exploited). On the other hand, the massive cluster ω Cen was not checked as a possible candidate, because it was not included in the Noyola & Gebhardt (2006) sample, and moreover, small slopes in the core region could not be revealed in published SB profiles (e.g. Meylan 1987; Ferraro et al. 2006).

Nonetheless, a recent and accurate determination of the ω Cen centre and the use of HST/ACS images led Noyola et al. (2008) to detect a steeper profile in the core region of this peculiar cluster, thus suggesting the influence of an IMBH. By fitting the high inner peak of the line-of-sight velocity dispersion (LOSVD) found from Gemini GMOS/IFU integrated light spectroscopy ($= 23 \pm 2 \text{ km s}^{-1}$ at an average radius $\sim 1''.9$) with non-parametric and orbit-based models with uniform mass-to-light ratio, Noyola et al. estimate a $\sim 4 \times 10^4 M_{\odot}$ object residing at the cluster centre. However, by solving the spherical and anisotropic Jeans equation on the Anderson & van der Marel (2010) projected density and kinematic data, van der Marel & Anderson (2010) find that the presence of an IMBH is possible only if $M_{\bullet}/M \lesssim 4.3 \times 10^{-3}$, which corresponds to about half the mass predicted by Noyola et al.

In this paper we would like to provide further evidence on the presence of the IMBH and to give another independent estimate of its mass, by means of a parametric fitting of both the SB and the LOSVD profiles using the M07 model. The results from the best fit of the SB profile are described in Sect. 2, while those coming from the LOSVD fitting are presented in Sect. 3. Concluding remarks are reported in Sect. 4.

2. The fit of the surface brightness

To study the ω Cen SB profile, we considered the HST/ACS measurements recently made by Noyola et al. (2008) inside $40''$ from the cluster centre, while for outer radii we took the observations by Meylan (1987, their Table 1).

As is evident from the too low concentration of the dotted profile in Fig. 1 (bottom panel), we notice that the SM isotropic model is unable to fit the outermost part ($r \gtrsim 13'$) of the SB profile, where, however, the background contamination should be negligible, for it was shown to only be relevant for $r \gtrsim 33'$ (Leon et al. 2000). Thus, the discrepancy from the prediction of this model should be due to the intrinsic dynamical state of the cluster outskirts. In fact, we find that a good fit of the whole profile can be achieved by including either a certain degree of radial velocity anisotropy or an MM stellar population with mass segregation (keeping isotropic velocities).

Nevertheless, the fit of the inner SB profile with a SM isotropic model permitted us to determine the best fit value for M_{\bullet}/M regardless of velocity anisotropy, because the presence of the latter only influences the outer region (as happens in normal King-Michie models, see, e.g., Gunn & Griffin 1979; Mocchi 2006). Thus, a grid of SM isotropic models have been generated by sampling the form parameters W_{BH} and M_{\bullet}/M . As the model profiles are expressed in dimensionless units, they have to be scaled in both the radial and the SB dimension. Thus, for each model of the grid we found the best fit values for two suitable

¹ The model can also include velocity anisotropy in the GC outskirts. In this case the outer SB profile shape depends on the anisotropy radius, too.

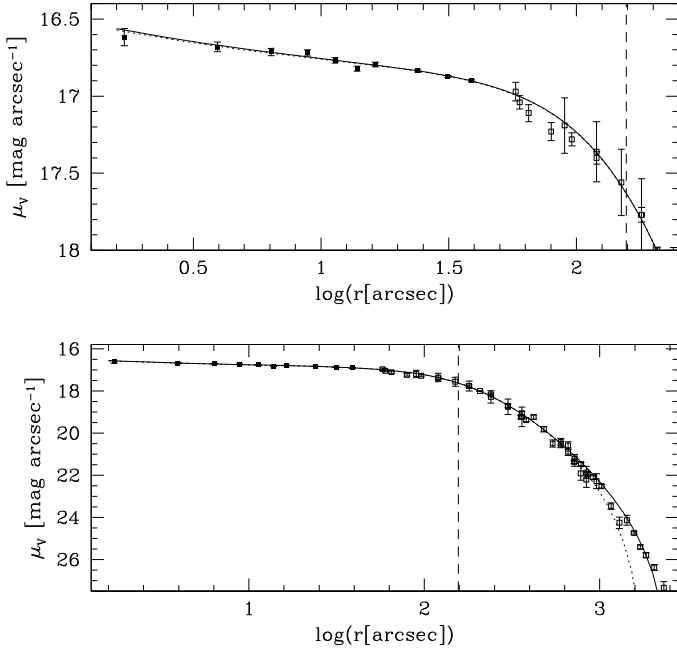


Fig. 1. *Bottom panel:* surface brightness profile of ω Cen and the SM isotropic (dotted line) and anisotropic (solid line; with $r_a = 4.5r_c$) best fit. In the case of the isotropic model, only data with $\log(r) < 2.9$ have been considered for the best fit search. The MM isotropic model yields a best fit profile that is indistinguishable from that given in the SM anisotropic case. For $\log(r) < 1.6$, the HST/ACS observations by Noyola et al. (2008) are used (filled squares), while for $\log(r) > 1.6$ data are taken from Meylan (1987, open squares). The *top panel* shows an enlarged view of the central region. The core radius is plotted with a dashed line.

scale parameters, namely the “visual” core radius² r_c and the normalisation value of the SB, restricting the fit to data points with $r < 13'2$. Since the SB measurements uncertainties are known, we minimised the χ^2 sum weighted by the width of the error bars.

The calculated χ^2 values are reported in Fig. 2, from which we deduce that $W_{\text{BH}} = 5.25$ and $M_{\bullet}/M = 5.8^{+0.9}_{-1.2} \times 10^{-3}$, with a level of confidence (LOC) of 68.3%. The best fit isotropic model gives $r_c = 156''$, which confirms both the more recent observations by Ferraro et al. (2006) and the value listed in Trager et al. (1995).

Once W_{BH} and M_{\bullet}/M has been determined by fitting the inner SB profile, we fit the entire data set by including radial velocity anisotropy in the stellar system outskirts (confirming what was already noted by Meylan 1987), namely outside an anisotropy radius r_a ; see, e.g., Miocchi (2006) for a description of how anisotropic velocities can be efficiently implemented in King-Michie models. Thus, a “sub-grid” of anisotropic models is generated by sampling r_a in the range $[2, 10] \times r_c$. The resulting χ^2 behaviour, this time evaluated over all SB data, is plotted in Fig. 3 and leads to the estimates $r_a = (4.5 \pm 0.1) \times r_c = 12' \pm 0'2$ with an LOC of 68.3%. From this figure, it can also be noted how the anisotropic model when “pushed” towards the isotropic case ($r_a \gg r_c$) gives unacceptable fits (huge χ^2 values). van de Ven et al. (2006) find that the velocity distribution in ω Cen is nearly isotropic inside $\sim 10'$, in agreement to our best fit value for r_a .

² Here r_c is defined as the radius at which the SB drops to half its value at r_{cu} . In good approximation, r_c coincides with the location of the “turn-off” of the profile (also called “break radius” in Noyola & Gebhardt 2006; see M07 for more details).

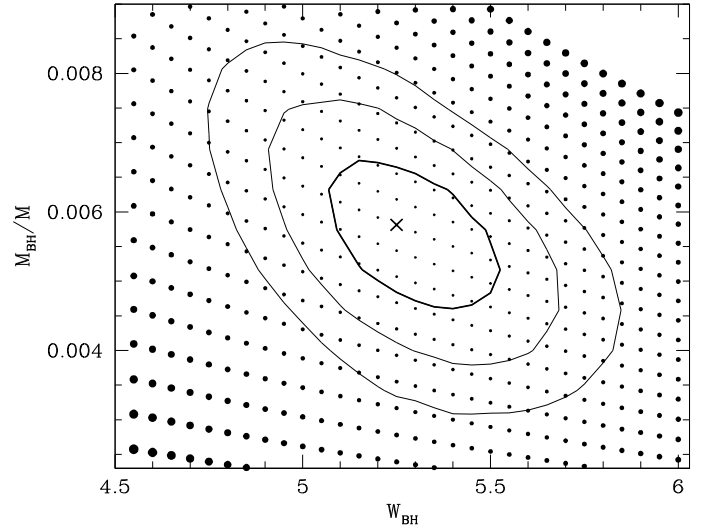


Fig. 2. Contours of χ^2 as a function of W_{BH} and of the M_{\bullet}/M ratio, plotted for the grid of SM isotropic models (the filled dots, with size proportional to χ^2) fitted to data points with $r < 13'2$. The central cross marks the minimum χ^2 model location ($W_{\text{BH}} = 5.25$ and $M_{\bullet}/M = 5.8 \times 10^{-3}$) and the isocontours for $\Delta\chi^2 = 2.3, 6.17, 11.8$ correspond to confidence regions of 68.3 (thick line), 95.4, and 99.7%, respectively.

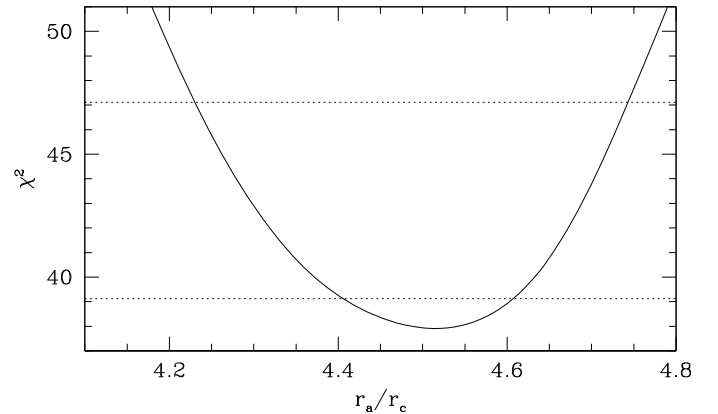


Fig. 3. χ^2 behaviour of the best fit SM model in the isotropic case (the cross in Fig. 2) when anisotropy is introduced, as a function of the anisotropy radius r_a . In this case, all the available SB data are taken into account. The χ^2 values (for $\Delta\chi^2 = 1, 9$) corresponding to an LOC of 68.3 and 99.7% are also plotted (dotted lines).

On the other hand, these authors reported the presence of a slight tangential anisotropy in the cluster outskirts which is, however, below the uncertainty in the velocity dispersion measurements (see their Fig. 8).

The SM anisotropic best fit model reported in Fig. 1 yields a tidal radius $r_t = 41'3$ and a concentration parameter, $c = \log(r_t/r_c) \approx 1.2$, substantially lower than the 1.6 value quoted in the Harris (1996) catalogue, but in good agreement with recent results (Ferraro et al. 2006; van de Ven et al. 2006).

As we said at the beginning of this section, the entire observed SB profile can also be fitted fairly well by an MM isotropic model (see also Meylan 1987) including the IMBH and stars in the mass range $0.4\text{--}1.2 M_{\odot}$ distributed following the Salpeter mass function, with central energy equipartition. In this case, the best fit profile is for $M_{\bullet}/M = 2.8 \times 10^{-3}$ (and $W_{\text{BH}} = 7.5$), and it practically overlaps with that of the anisotropic case (Fig. 1). Nonetheless, we discarded this MM

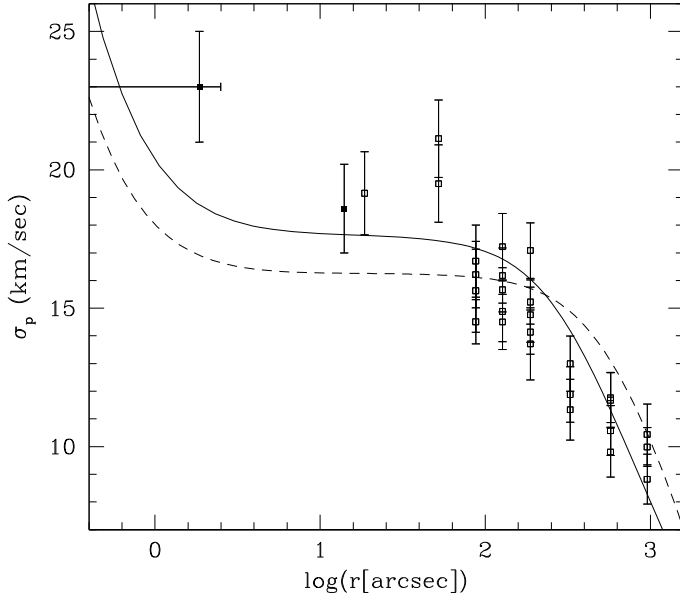


Fig. 4. Best fit LOSVD radial profile in the SM anisotropic (solid line) and MM isotropic case (dashed line; in this case, it is determined by weighting the contributions of all the stellar components according to their luminosity). The best fit total cluster mass is 3.1 and $4.4 \times 10^6 M_{\odot}$, respectively. Filled squares are the measurements from Noyola et al. (2008), open squares come from van de Ven et al. (2006).

model because it underestimates the LOSVD in the central region, as we see in detail in next section.

3. Velocity dispersion profile

To provide an estimate of M_{\star} , we have to quantify the cluster total mass M first. This can be done by exploiting the most recent kinematic observations of ω Cen. For this purpose, along with the two innermost points taken from the Gemini GMOS-IFU measurements in Noyola et al. (2008), we use the LOSVD data employed by van de Ven et al. (2006, see references therein for the discussion of the various data sources). These are based on various independent sets of measurements, which in most of the radial annuli include values taken in different apertures (see Fig. 4). A radial error bar is plotted for the innermost point to indicate the width of the $5'' \times 5''$ GMOS-IFU field of view that was centred on the cluster nucleus to obtain the integrated spectrum (Noyola et al. 2008).

Once the SB profile has been fitted, the *form* of the LOSVD profile is univocally given by the model and cannot be adapted to the observed behaviour. The best fit can be found by adjusting only the velocity scale factor (corresponding to a vertical shifting of the profile). In turn, this factor depends on the adopted cluster distance and total mass M . We chose to a-priori fix the distance to 4.8 kpc (as from van de Ven et al. 2006), and then to find the M value that gives the best fit to the LOSVD observations. Shown in Fig. 4 are two LOSVD best fit profiles: the one given by the SM anisotropic model and the one produced by the MM isotropic one.

It is evident (see also Fig. 5) that the SM case yields a better fit to LOSVD data, having $P(\chi^2 > \chi_{\text{fit}}^2) = 84\%$, compared with the MM model that gives $P(\chi^2 > \chi_{\text{fit}}^2) = 47\%$ mainly because, in the inner region ($\log r < 1.8$), it exhibits too low an LOSVD. This is naturally expected from the mass distribution in the MM case being dominated by the lighter (and fainter) stars, which are much less concentrated than the giants. Thus, the velocity

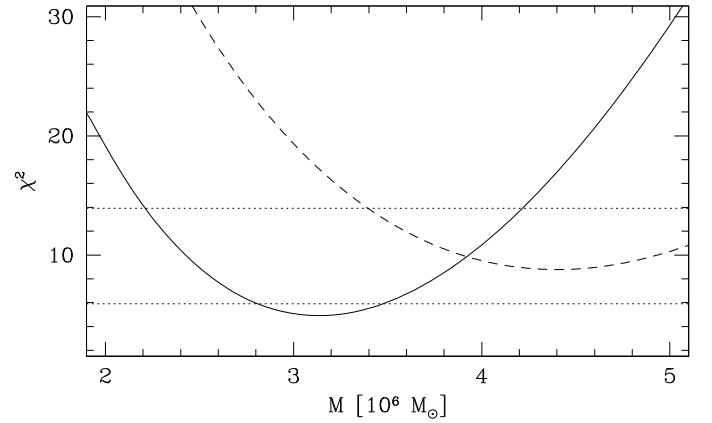


Fig. 5. χ^2 behaviour of the LOSVD fit as a function of the total cluster mass M in the SM anisotropic (solid line) and MM isotropic (dashed) case. The dotted lines indicate the 68.3 and 99.7% LOC.

dispersion of the giants starts to decrease at larger radii, consequently the best fit tends to give a lower inner LOSVD in the attempt to fit the outer data. Interestingly, that the SM model better represents the dynamical situation of this cluster suggests that mass segregation has not been efficient in ω Cen. In this sense, it confirms the current thought that this cluster is not completely relaxed by collisions, because of its relatively long relaxation time (see, e.g., Meylan 1987; Meylan et al. 1995). Various authors, indeed, have found indications of a uniform mass-to-light ratio (see, e.g., Merritt et al. 1997; van de Ven et al. 2006).

Considering the relatively large error bars of LOSVD measurements in crowded regions, from Fig. 4 we note that the model profile predicts that the central velocity cusp is apparently more centrally concentrated than Noyola et al. (2008) observations suggest (it starts to be evident only for $r \lesssim 1''$), though one has to consider the “visual effect” of the logarithmic scale in r . In fact, a relatively large residual ($\sim 4 \text{ km s}^{-1}$) still remains for the innermost LOSVD data point, although its radial error bar intersects the model profile (at $r \approx 0''.6$). If the M07 model represents the real cluster dynamical state well, this could indicate the influence of some statistical bias affecting this bin or too large an average radius chosen for it. In this respect, it is also worth noting that recent and accurate proper motion measurements reveal no significant velocity cusp at the central region of this cluster, though this study relies on a different dataset and kinematic centre location and, moreover, the authors do not observe any appreciable cusp in density (Anderson & van der Marel 2010).

In Noyola et al. (2008) the innermost bins are fitted quite well (apart from the measurement at $\log(r) \approx 1.7$, see their Fig. 4). However, it must be noticed that in these authors’ model the IMBH mass best fit value depends almost completely on the few innermost LOSVD data points, while it has practically no effects for $r \geq 30''$ and plays no role at all on the SB profile. In our case, on the contrary, the behaviour of the LOSVD given by the model is strongly dependent on the best fit parameters of the SB profile. If our model were forced to fit the entire LOSVD well, then the required $\sim 4 \times 10^4 M_{\odot}$ IMBH would produce a much steeper SB core behaviour (along with too low a concentration), which would be completely different from the observed one. The disadvantage of our parametric approach is that it is “less general”, because it is constrained by the theoretical hypothesis lying behind the assumption of that particular distribution function in phase-space.

The predicted cluster total mass is $M = (3.1 \pm 0.3) \times 10^6 M_{\odot}$ with an LOC of 68.3% (Fig. 5). It is in marginal agreement with

the dynamical estimate of $(2.5 \pm 0.3) \times 10^6 M_{\odot}$ in [van de Ven et al. \(2006\)](#) – though it would agree well at 2σ level – while much lower than the [Meylan \(1987\)](#) $3.9 \times 10^6 M_{\odot}$ value. This author used a King-Michie MM model in which an approximated energy equipartition was imposed (see [Miocchi 2006](#), for a discussion of this approximation). This, together with the assumed presence of very low-mass stars (down to $0.13 M_{\odot}$), can explain the higher M estimate. As far as the M/L ratio is concerned, if one assumes a total V -band luminosity in the “prudential” range $L_V = (1.0 \pm 0.2) \times 10^6 L_{\odot}$ (e.g. [Seitzer 1983](#); [Meylan 1987](#); [Carraro & Lia 2000](#)), one gets $M/L_V = 3.1 \pm 0.9$, a value compatible with the accurate 2.5 ± 0.1 [van de Ven et al. \(2006\)](#) estimate. Of course, as the model predicts no mass segregation, the mass-to-light ratio turns out to be uniform.

The estimate made in Sect. 2 of the ratio M_{\bullet}/M , combined with the uncertainty on the cluster total mass, yields an IMBH mass in the range $1.3 \times 10^4 < M_{\bullet} < 2.3 \times 10^4 M_{\odot}$ (with a 68.3% LOC), which spans about one third to a half the mass predicted by [Noyola et al. \(2008\)](#), but is marginally compatible with the $\leq 1.3 \times 10^4 M_{\odot}$ [van der Marel & Anderson \(2010\)](#) estimate. However, it has to be kept in mind that these two estimates rely on different cluster centre. Finally, it is worth noting how our estimate range, though still incompatible, gets closer to the $\sim 2300 M_{\odot}$ upper limit as constrained by the ω Cen radio continuum emission ([Maccarone & Servillat 2008](#)).

4. Conclusions

In this paper we have presented a parametric fit of the surface brightness (SB) profile of ω Cen (NGC 5139), made up of HST/ACS data in the central region ([Noyola et al. 2008](#)) and of the [Meylan \(1987\)](#) normalised profile in the outskirts. The fit was done by using a self-consistent (spherical and non-rotating) model that includes a central intermediate-mass black hole (IMBH). The whole SB profile (from $r \sim 1'6$ out to $r \sim 42'$) can be well-fitted by the model both with the single-mass stellar distribution – assuming a radially anisotropic velocity distribution outside $12'$ – and with a multimass model with isotropic velocity. The comparison of the generated LOSVD with the kinematic observations recently enriched at the very central region by Gemini GMOS-IFU measurements ([Noyola et al. 2008](#)), however, allows this degeneracy to be resolved in favour of the single-mass case. In fact, the multimass model yields too low an LOSVD in the central region. This suggests that ω Cen is presently in a non mass-segregated state, as already argued by various authors (e.g. [Meylan 1987](#); [Meylan et al. 1995](#); [van de Ven et al. 2006](#)). It is also worth noting that recent N -body studies show that the presence of an IMBH in a cluster can suppress mass segregation ([Gill et al. 2008](#)).

From this parametric study we deduce the 68.3% confidence intervals $M = (3.1 \pm 0.3) \times 10^6 M_{\odot}$ for the cluster total mass and $M_{\bullet}/M = 5.8_{-1.2}^{+0.9} \times 10^{-3}$ for the mass ratio, leading to an estimate for the IMBH mass in the range $13\,000 < M_{\bullet} < 23\,000 M_{\odot}$. This value is from about one third to a half the $\sim 40\,000 M_{\odot}$ mass predicted by [Noyola et al. \(2008\)](#), though it is compatible with the $13\,000 M_{\odot}$ upper limit provided by the dynamical analysis in [van der Marel & Anderson \(2010\)](#). Note, however, that these two published estimates are based on different cluster centre.

Acknowledgements. The author is warmly grateful to Dr. B. Lanzoni and Dr. E. Noyola for helpful discussions and suggestions. The paper presentation greatly benefited from the comments of the anonymous referee.

References

- Anderson, J., & van der Marel, R. P. 2010, *ApJ*, 710, 1032
 Bahcall, J. N., & Wolf, R. A. 1976, *ApJ*, 209, 214
 Baumgardt, H., Makino, J., & Ebisuzaki, T. 2004, *ApJ*, 613, 1133
 Baumgardt, H., Makino, J., & Hut, P. 2005, *ApJ*, 620, 238
 Binney, J. J., & Tremaine, S. 1987, *Galactic Dynamics* (Princeton, NJ: Princeton Univ. Press)
 Carraro, G., & Lia, C. 2000, *A&A*, 357, 977
 Faber, S. M., Dressler, A., Davies, R. L., Burstein, D., & Lynden-Bell, D. 1987, in *Nearly Normal Galaxies: From the Planck time to the present*, ed. S. M. Faber (New York: Springer), 175
 Faber, S. M., & Jackson, R. E. 1976, *ApJ*, 204, 668
 Ferrarese, L., & Merritt, D. 2000, *ApJ*, 539, L9
 Ferraro, F. R., Sollima, A., Rood, R. T., et al. 2006, *ApJ*, 638, 433
 Freitag, M., & Benz, W. 2002, *A&A*, 394, 345
 Gebhardt, K., Bender, R., Bower, G., et al. 2000, *ApJ*, 539, L13
 Gebhardt, K., Rich, R. M., & Ho, L. C. 2005, *ApJ*, 634, 1093
 Gill, M., Trenti, M., Miller, C. M., et al. 2008, *ApJ*, 686, 303
 Gunn, J. E., & Griffin, R. F. 1979, *AJ*, 84, 752
 Harris, W. E. 1996, *AJ*, 112, 1487
 King, I. R. 1966, *AJ*, 71, 64
 Kong, A. K. H., Heinke, C. O., Di Stefano, R., et al. 2009, *ApJL*, submitted [arXiv:0910.3944]
 Ibata, R. A., Bellazzini, M., Chapman, S. C. et al. 2009, *ApJ*, 699, L169
 Irwin, J. A., Brink, T., Bregman, J. N., & Roberts, T. P. 2010, *ApJ*, 712, L1
 Lanzoni, B., Dalessandro, E., Ferraro, F. R., et al. 2007, *ApJ*, 668, L139
 Leon, S., Meylan, G., & Combes, F. 2000, *A&A*, 359, 907
 Liu, J., & Di Stefano, R. 2008, 10th HEAD meeting of the American Astronomical Society, 1, 14
 Maccarone, T. J., & Servillat, M. 2008, *MNRAS*, 389, 379
 Magorrian, J., Tremaine, S., Richstone, D., et al. 1998, *AJ*, 115, 2285
 Meylan, G. 1987, *A&A*, 184, 144
 Meylan, G., & Heggie, D. C. 1997, *A&AR*, 8, 1
 Meylan, G., Mayor, M., Duquennoy, A., & Dubath, P. 1995, *A&A*, 303, 761
 Merritt, D., Meylan, G., & Mayor, M. 1997, *AJ*, 114, 1074
 Michie, R. W. 1963, *MNRAS*, 125, 127
 Michie, R. W., & Bodenheimer, P. 1963, *MNRAS*, 126, 269
 Miller, C. M., & Colbert, E. J. M. 2004, *Int. J. Mod. Phys. D*, 13, 1
 Miocchi, P. 2006, *MNRAS*, 366, 227
 Miocchi, P. 2007, *MNRAS*, 381, 103 (M07)
 Noyola, E., & Gebhardt, K. 2006, *AJ*, 132, 447
 Noyola, E., Gebhardt, K., & Bergmann, M. 2008, *ApJ*, 676, 1008
 Nucita, A. A., De Paolis, F., Ingrassio, G., Carpano, S., & Guainazzi, M. 2008, *A&A*, 478, 763
 Pooley, D., & Rappaport, S. 2006, *ApJ*, 644, L45, 2006
 Preto, M., Merritt, D., & Spurzem, R. 2004, *ApJ*, 613, L109
 Safonova, M., & Shastri, P. 2010, *Ap&SS*, 325, 47
 Seitzer, P. O. 1983, Ph.D. Thesis, Australian National Univ.
 Servillat, M., Dieball, A., Webb, N. A., et al. 2008, *A&A*, 490, 641
 Soria, R., Hau, G. K. T., Graham, A. W., et al. 2010, *MNRAS*, accepted [arXiv:0910.1356]
 Strohmayer, T. E., & Mushotzky, R. F. 2009, *ApJ*, 703, 1386
 Trager, S. C., King, I. R., & Djorgovski, S. 1995, *AJ*, 109, 218
 Trenti, M., Ardi, E., Mineshige, S., & Hut, P. 2007, *MNRAS*, 374, 857
 Trenti, M., Vesperini, E., & Pasquato, M. 2010, *ApJ*, 708, 1598
 Ulvestad, J. S., Greene, J. E., & Ho, L. C. 2007, *ApJ*, 661, L151
 Umbreit, S., Fregeau, J. M., & Rasio, F. A. 2009, *ApJ*, submitted [arXiv:0910.5293]
 van de Ven, G., van den Bosch, R. C. E., Verolme, E. K., & de Zeeuw, P. T. 2006, *A&A*, 445, 513
 van der Marel, R. P., & Anderson, J. 2010, *ApJ*, 710, 1063
 Zepf, S. E., Stern, D., Maccarone, T. J., et al. 2008, *ApJ*, 683, L139